A scattering analysis for homogeneous sphere model by FDTD method with a new improved PML absorbing boundary condition: Application to uniaxial-pseudo propagation PML

***Kensuke Sasaki**, Yukihisa Suzuki, Masao Taki*

Dept. of Electrical & Electronic Engineering, Tokyo Metropolitan Univ., Tokyo, Japan,
sasaki@com.eei.metro-u.ac.jp

Abstract

A new improved PML called as uniaxial-pseudo propagation PML (UPP-PML) was proposed for the purpose to reduce computational costs from the conventional Berenger's PML (B-PML). The UPP-PML is a new absorbing boundary condition for finite difference time-domain (FDTD) method. In our past study, propagation and absorbing ability without scattering object were investigated for the UPP-PML. In this study, we applied the UPP-PML to the FDTD method in scattering analysis. The scattering analysis for homogeneous sphere model with plane wave injection was evaluated as a case study. The distributions of effective value for electric field in the stationary state were evaluated. The numerical results with the UPP-PML were compared with those of exact solution and the conventional B-PML. It was found that the distributions of the effective value obtained with the UPP-PML were almost as same as those with the conventional B-PML result. Consequently, scattering analysis with the UPP-PML had almost as same calculation accuracy as the B-PML. Furthermore, using the UPP-PML made advantage in reduced computational costs over the B-PML.

1. Introduction

The conventional perfectly matched layer [1] (PML) absorbing boundary condition (ABC), which is used for electromagnetic field analysis by the finite difference time-domain (FDTD) method, has the high absorbing ability. The conventional PML-ABCs, such as the Berenger's PML (B-PML) or the uniaxial PML, require for many computational costs. In past study, several modified PML schemes had been proposed for the purpose to reduce computational costs from the conventional PML-ABCs [2-4]. A new improved PML scheme called as uniaxial-pseudo propagation PML [5-6] (UPP-PML) was developed in our recent works. Here, propagation and absorbing ability without scattering object were investigated for the UPP-PML. In the recent study, it was found that the UPP-PML has almost as same absorbing ability as the conventional PML-ABCs and advantage in reduced computational costs over the conventional PML-ABCs.

The purpose of this study is to evaluate the UPP-PML in practical analysis. The UPP-PML was applied to the FDTD method in scattering analysis for homogeneous sphere model. Distributions of effective value for electric field in stationary state obtained by the UPP-PML were evaluated. In this evaluation, the results from the UPP-PML were compared with those of the exact solution [7] and the conventional Berenger's PML.

2. Concept for the UPP-PML

The UPP-PML is a new improved PML-ABC, which applied UPP concept [5] for multi-dimensional wave propagation scheme in the PML region. Here the UPP concept is introduced by comparing with the conventional split field [1] (SF) concept. Figure 1(a) and (b) show the wave propagation concepts for the SF and the UPP, respectively. These figures indicate the wave propagation for z component of electric wave E_z on the cross section of x-y plane from n to n+1. Here, n indicates number of time steps from initial condition. In the SF concept, E_z is split into subcomponents E_{zx} and E_{zy}, as shown in Fig. 1(a). As the figure shows, E_{zx} and E_{zy} propagate along x and y axes during time proceeding from n to n+1, respectively. E_z at n+1 is calculated by the sum of E_{zx} and E_{zy} at n+1. On the other hands, E_z propagation is split into x and y directions via n' in the UPP concept, as shown by the solid arrows (b-1) and (b-2) in Fig. 1(b). Here n' is introduced as pseudo-time step between n and n+1. First, E_z propagates along x direction from n to n'. Then, E_z propagates along y direction from n' to n+1. According to the UPP concept, time proceeding for the wave propagation during n to n+1 is split into two steps.

Differences between the UPP and the SF concepts in computational costs are discussed as follows [5-6]. In the focusing on the required memories, the SF requires to memorize three values, which are E_z, E_{zx}, and E_{zy} in each time steps. On the other hands, the UPP requires to memorize only one value E_z, because E_z value in the memory is sequentially renewed following order as $E_z^{n} \rightarrow E_z^{n'} \rightarrow E_z^{n+1}$ on the process of time proceeding for the propagation from n to n+1. Consequently, required memories are saved to 1/3 from the SF scheme by using the UPP scheme. In focusing on the calculation time, the SF requires a sum up operation in order to derive E_z from two subcomponents E_{zx} and E_{zy} at n+1. Because the calculation time is depends on the number of operators, the calculation time of the UPP is reduced from the SF.

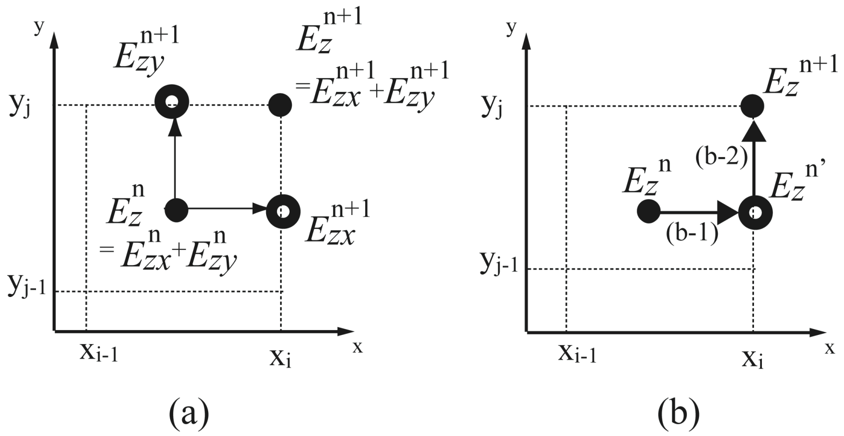

Fig. 1: The propagation concept of E_z from n to n+1. (a) The concept for the split field. (b) The concept for the UPP.

3. Formulation for the UPP-PML

In this section, the formulation of the UPP-PML is introduced [5-6]. To avoid repetition, the formulation for updating E_z is shown in eqs. (1a) and (1b). Here, H_x and H_y indicate x and y components for magnetic field, and ε indicates electric permittivity. σ_x and σ_y indicate electric conductivities along x and y axes, respectively. Equations (1a) and (1b) correspond to one-dimensional wave propagations along x and y directions, respectively. The discretizations of $\partial E_z/\partial t$ are shown in eqs. (1a) and (1b) by introducing pseudo-time step n'. The space differentials in eqs. (1a) and (1b) are discreted as same manner as the conventional FDTD method.

$$\varepsilon \frac{\partial}{\partial t} E_z \Big|_{t=n\Delta t} \cong \varepsilon \frac{E_z^{n'} - E_z^{n}}{\Delta t} = \frac{\partial}{\partial x} H_y^{n} - \sigma_x \frac{E_z^{n'} - E_z^{n}}{2} \tag{1a}$$

$$\varepsilon \frac{\partial}{\partial t} E_z \Big|_{t=n\Delta t} \cong \varepsilon \frac{E_z^{n+1} - E_z^{n'}}{\Delta t} = -\frac{\partial}{\partial y} H_x^{n} - \sigma_y \frac{E_z^{n+1} - E_z^{n'}}{2} \tag{1b}$$

4. Scattering analysis

In this study, the UPP-PML was applied for scattering analysis with the FDTD method to evaluate calculation accuracy in the numerical solution. The conditions for the simulation were as follows. Figure 2 shows schematic view of calculation model for scattering analysis with the homogeneous dielectric sphere. The calculation region was 0.5 m×0.5 m×0.5 m. The radius of sphere model was 0.1 m, and the center of the sphere was located on the origin of the Cartesian coordinate O. The relative permittivity, relative permeability, and electric conductivity in the sphere were 40, 1, and 1 S/m, respectively. The outer region of the sphere was vacuum condition. The voxel size and time step were 5 mm and 2 ps, respectively. The wave source was 1 GHz plane wave which propagates along x axis toward positive direction, and its amplitude was 1 V/m.

The PML region was inserted at the outside of the calculation region. The electric conductivity for PML $\sigma_j(i)$ is defined by eq. (2) [1]. Here $\sigma_j(i)$ is function of i. i, A and L are position number within the PMLs, maximum electric conductivity, and number of the PMLs, respectively. i=1 indicates location of inner surface of the PML, and i=L indicates that of outer surface of the PML. The increase ratio of $\sigma_j(i)$ is decided by the value of the M. Here, A, L, and M

were 1 S/m, 10 layers, and 3 in this study. The conditions of $\sigma_j(i)$ used in the B-PML was as same as those of the UPP-PML. The simulation was carried out during 5 periods to obtain the numerical results in the stationary state.

$$\sigma_j(i) = A(i/L)^M \qquad j = x, y, z \tag{2}$$

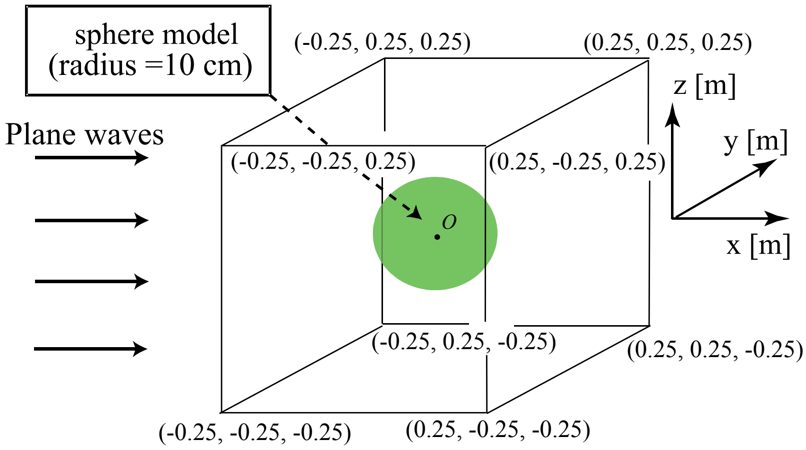

Fig. 2: The schematic view of the calculation model.

5. Results

Effective values of electric field $|E|_{rms}$ all over the calculation region in the stationary state were evaluated by comparing with those of the conventional B-PML result. Figure 3 indicates the $|E|_{rms}$ distributions on the *x-y* cross-section at z=0. The $|E|_{rms}$ distributions of all calculation region were shown in this figure. Here, Fig. 3(a) and (b) indicate the $|E|_{rms}$ distributions calculated with the B-PML and the UPP-PML, respectively. There were no significant differences in the $|E|_{rms}$ distributions between the B-PML and the UPP-PML results all over the calculation region, as shown in Figs. 3(a) and (b).

Accuracies of the numerical results in the sphere were evaluated by comparing with the exact solution [7]. The $|E|_{rms}$ distributions within the sphere were shown in Fig. 4. Here, Fig. 4 (a), (b) and (c) indicate the distributions calculated with the B-PML, the UPP-PML, and obtained by the exact solution, respectively. The $|E|_{rms}$ distributions within the sphere calculated with the B-PML and the UPP-PML were almost as same as those of the exact solution. Relative errors from the exact solution for spacial average of the $|E|_{rms}$ in the sphere, which obtained by the B-PML and the UPP-PML, were 4.2% and 3.9%, respectively. Relative errors for maximum value of the $|E|_{rms}$ in the sphere, which obtained by the B-PML and the UPP-PML, were 16.0% and 15.7%, respectively. In this case study, the required memory of the UPP-PML was 56% less than that of the B-PML in the whole calculation. The calculation time of the UPP-PML was 10% less than that of the B-PML, too.

5. Conclusion

In this study, we applied the UPP-PML to the FDTD method in the scattering analysis. The scattering analysis for the homogeneous sphere model with plane wave injection was performed as a case study. The effective values of electric field $|E|_{rms}$ in the stationary state obtained with the UPP-PML were evaluated by comparing with those obtained by using the conventional B-PML. As a result, the $|E|_{rms}$ distributions with the UPP-PML were almost as same as those with the B-PML. The $|E|_{rms}$ distributions inside the sphere were also compared with those of the exact solution. The relative errors for spacial average of the $|E|_{rms}$ in the sphere obtained with the both ABCs were about 4%. The relative errors for maximum value of the $|E|_{rms}$ in the sphere obtained by the both ABCs were about 16.0%. These results indicate that scattering analysis with the UPP-PML had almost as same calculation accuracy as the B-PML. Furthermore, the computational costs of the UPP-PML were smaller than those of the B-PML. The UPP-PML had advantage over the B-PML in scattering analysis.

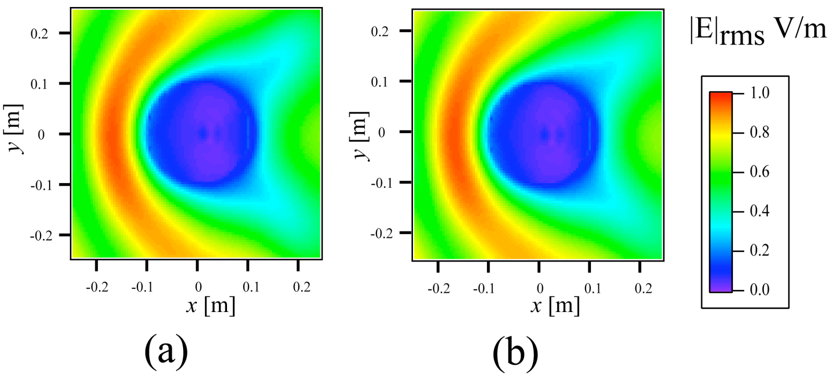

Fig. 3: The $|E|_{rms}$ distributions on the *x-y* cross-section at *z*=0. (a) B-PML (b) UPP-PML

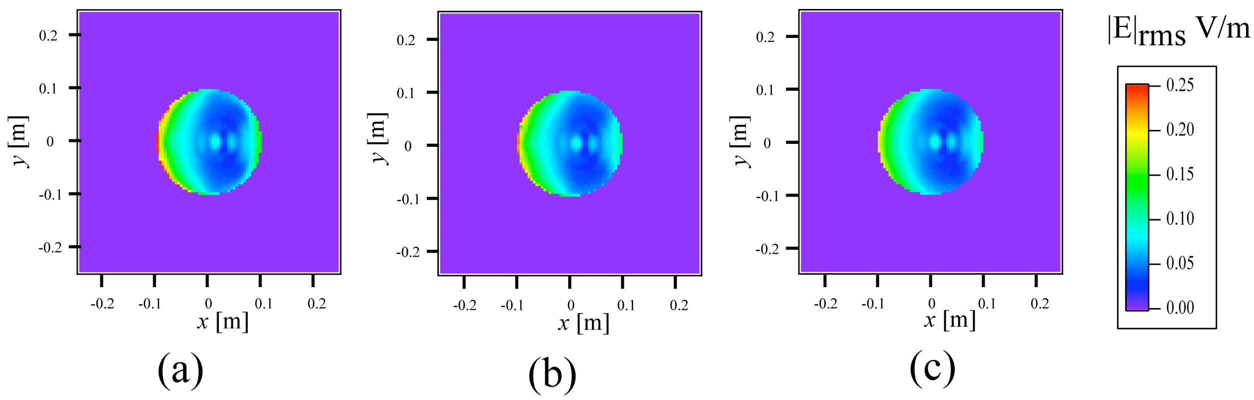

Fig. 4: The $|E|_{rms}$ distributions on the *x-y* cross-section at z=0 inside the sphere.
(a) B-PML (b) UPP-PML (c) exact solution

7. References

1. A. Taflove, S. C. Hagness, "Computational electromagnetics the finite difference time domain method", Artech House INC, Norwood, 2005

2. J. C. Veihl, R. Mittra, "An efficient implementation of Berenger's perfectly matched layer (PML) for finite-difference time-domain meth transaction", IEEE Microwave and Guided Wave Letters, vol. 6, No. 2, pp. 94-96, February, 1996

3. D. M. Sullivan, "An unsplit step 3-D PML for use with the FDTD method", IEEE Microwave and Guided Wave Letters, vol. 7, No. 7, pp. 184-186, February, 1997

4. T. Yu, B. Zhou, and B. Chen, "An unsplit formulation of the Berenger's PML absorbing boundary condition for FDTD meshes", IEEE Microwave and Guided Wave Letters, vol. 13, No. 8, pp. 348-350, August, 2003

5. K. Sasaki, Y. Suzuki, M. Taki, “Applying uniaxial-pseudo propagation scheme to PML absorbing boundary condition for reducing computational costs”, C-Abstracts of IEICE Transactions on Electronics, Vol. J90-C, No. 7, pp. 577-578, 2007, in Japanese

6. K. Sasaki, S. Suzuki, and M. Taki, “Reduction of computational costs in FDTD simulation with a new ABC based on PML for large scale dosimetry”, Bioelectromagnetics society, Kanazawa, Japan, 2007

7. J. J. Bowman, “Electromagnetic and Acoustic Scattering by Simple Shapes”, Hemisphere Pub. , 1987